Ectopic Expression of *WRINKLED1* Affects Fatty Acid Homeostasis in *Brachypodium distachyon* Vegetative Tissues[1][OPEN]

Yang Yang, Jacob Munz[2], Cynthia Cass, Agnieszka Zienkiewicz, Que Kong, Wei Ma, Sanjaya[3], John Sedbrook, and Christoph Benning*

Department of Biochemistry and Molecular Biology (Y.Y., A.Z., Q.K., C.B.), Great Lakes Bioenergy Research Center (Y.Y., J.M., C.C., A.Z., Q.K., W.M., S., J.S., C.B.), and Department of Plant Biology (W.M.), Michigan State University, East Lansing, Michigan 48824; School of Biological Sciences, Illinois State University, Normal, Illinois 61790 (J.M., C.C., J.S.); and Michigan State University-Department of Energy Plant Research Laboratory, East Lansing, Michigan 48824 (Y.Y., A.Z., Q.K., W.M., C.B.)

ORCID ID: 0000-0001-8585-3667 (C.B.).

Triacylglycerol (TAG) is a storage lipid used for food purposes and as a renewable feedstock for biodiesel production. WRINKLED1 (WRI1) is a transcription factor that governs fatty acid (FA) synthesis and, indirectly, TAG accumulation in oil-storing plant tissues, and its ectopic expression has led to TAG accumulation in vegetative tissues of different dicotyledonous plants. The ectopic expression of *BdWRI1* in the grass *Brachypodium distachyon* induced the transcription of predicted genes involved in glycolysis and FA biosynthesis, and TAG content was increased up to 32.5-fold in 8-week-old leaf blades. However, the ectopic expression of *BdWRI1* also caused cell death in leaves, which has not been observed previously in dicotyledonous plants such as Arabidopsis (*Arabidopsis thaliana*). Lipid analysis indicated that the free FA content was 2-fold elevated in *BdWRI1*-expressing leaf blades of *B. distachyon*. The transcription of predicted genes involved in β-oxidation was induced. In addition, linoleic FA treatment caused cell death in *B. distachyon* leaf blades, an effect that was reversed by the addition of the FA biosynthesis inhibitor cerulenin. Taken together, ectopic expression of *BdWRI1* in *B. distachyon* enhances FA biosynthesis and TAG accumulation in leaves, as expected, but also leads to increased free FA content, which has cytotoxic effects leading to cell death. Thus, while WRI appears to ubiquitously affect FA biosynthesis and TAG accumulation in diverse plants, its ectopic expression can lead to undesired side effects depending on the context of the specific lipid metabolism of the respective plant species.

Triacylglycerol (TAG) derived from seed oil is used as a vegetable oil but can also serve as a renewable source for biofuels and chemicals with industrial applications (Durrett et al., 2008). An extensive knowledge of TAG biosynthesis pathways and its molecular regulation has been developed as reviewed previously (Santos-Mendoza et al., 2008; Baud and Lepiniec, 2010; Bates et al., 2013). Arabidopsis (*Arabidopsis thaliana*) *WRINKLED1* (*AtWRI1*; At3g54230) encodes a transcription factor with two APETALA2 (AP2) DNA-binding domains and promotes the conversion of sugars to oil by directly activating genes encoding proteins involved in plastid glycolysis and fatty acid (FA) synthesis (Baud et al., 2009; Maeo et al., 2009; Fukuda et al., 2013). The Arabidopsis *wri1* mutant has an 80% reduction of seed oil content (Focks and Benning, 1998), whereas overexpression of *WRI1* increases seed oil content by 10% to 20% (Cernac and Benning, 2004). *WRI1* orthologs from maize (*Zea mays*), rape (*Brassica napus*), and oil palm (*Elaeis guineensis*) have been shown to be involved in TAG production in embryos or fruit mesocarps, and their overexpression leads to increased seed oil content (Liu et al., 2010; Shen et al., 2010; Pouvreau et al., 2011; Ma et al., 2013; van Erp et al., 2014). Ectopic expression of *WRI1* has also been used to stimulate oil production in nonseed tissues in both Arabidopsis and tobacco (*Nicotiana tabacum*; Cernac and Benning, 2004; Sanjaya et al., 2011; Dussert et al., 2013; Kelly et al., 2013;

[1] This work was supported by the U.S. Department of Energy Great Lakes Bioenergy Research Center Cooperative (grant no. DE–FC02–07ER64494) and by Michigan State University AgBioResearch.

[2] Present address: Department of Botany, Faculty of Science, 3529–6270 University Blvd., Vancouver, BC, Canada V6T 1Z4.

[3] Present address: Department of Biology, 101 Hamblin Hall, West Virginia State University, Institute, WV 25112.

* Address correspondence to benning@msu.edu.

The author responsible for distribution of materials integral to the findings presented in this article in accordance with the policy described in the Instructions for Authors (www.plantphysiol.org) is: Christoph Benning (benning@msu.edu).

Y.Y. designed and performed the experiments, analyzed the data, and wrote the first draft of the article; J.M., C.C., and A.Z. performed the experiments and analyzed the data; W.M. and Q.K. performed the screening and genotyping of *B. distachyon UBI*::*AtWRI1* transgenic plants; S. performed the screening and genotyping of Arabidopsis *35S*::*AtWRI1* transgenic plants; C.B. and J.S. supervised the study, designed the experiments, and analyzed the data; C.B. coordinated the writing and edited the drafts of the article.

[OPEN] Articles can be viewed without a subscription.

www.plantphysiol.org/cgi/doi/10.1104/pp.15.01236

Vanhercke et al., 2014; Grimberg et al., 2015; Ma et al., 2015).

During seed germination, the oxidation of FAs derived from TAGs provides energy for early seedling development (Graham, 2008). In addition to essential structural and nutritional functions, FAs and its derivatives also have many signaling functions. For instance, FAs are important signals in defense responses (Farmer et al., 1998; Kachroo et al., 2003; Chandra-Shekara et al., 2007). Very-long-chain FAs play a role in cell differentiation in Arabidopsis with their effect on polar auxin distribution (Roudier et al., 2010). Thus, overaccumulation of free FAs is expected to be detrimental to tissues. For example, exogenous and endogenous FAs are known to inhibit coleoptile elongation of oat (*Avena fatua*; Ando and Tsukamotoa, 1981; Ohkawa and Nishikawa, 1987), longitudinal cell growth of Arabidopsis (Li et al., 2011), axillary bud growth of tobacco (Tso, 1964), seedling growth of rice (*Oryza sativa*; Tsuzuki et al., 1987), and germination of lettuce (*Lactuca sativa*), oat, and mustard (*Sinapsis alba*; Le Poidevin, 1965; Berrie, 1979; Stewart and Berrie, 1979; Metzger and Sebesta, 1982). Furthermore, the accumulation of unsaturated FAs has been linked to cell death. Palmitoleic acid is reported to be an inducer of programmed cell death in tobacco and eggplant (*Solanum melongena*) protoplasts (Peters and Chin, 2005, 2007). Palmitoleic acid and linolenic acid cause the inhibition of photosynthetic electron transport, loss of thylakoid proteins, and release of cytochrome *f* in isolated chloroplasts from spinach (*Spinacia oleracea*) and eggplant (Golbeck and Warden, 1984; Warden and Csatorday, 1987; Peters and Chin, 2003). Increase of free FAs is the primary cause of chloroplast membrane damage and chlorophyll degradation and leads to necrosis when the Arabidopsis β-oxidation mutant *peroxisomal ABC-transporter1* is subjected to prolonged darkness (Kunz et al., 2009; Slocombe et al., 2009). Additionally, a recent study suggests that the proteins LIPIN, PHOSPHOLIPID: DIACYLGLYCEROL ACYLTRANSFERASE1 (PDAT1), and SUGAR-DEPENDENT1 (SDP1) function synergistically in Arabidopsis to protect plants against FA-induced cell death (Fan et al., 2013, 2014).

Brachypodium distachyon is an experimental model for temperate grasses and belongs to the family Poaceae (Draper et al., 2001; Opanowicz et al., 2008; Brkljacic et al., 2011). Recently, engineering the accumulation of TAG in vegetative tissues has been proposed for increasing the energy density of biomass crops (Ohlrogge and Chapman, 2011). Although significant investments have been made in developing and using *B. distachyon* as a model for biofuel crops (Brkljacic et al., 2011), little is known about its lipid metabolism pathways. In this study, we identified a *WRI1* ortholog of *B. distachyon*. Its role in FA biosynthesis and TAG accumulation in both storage and vegetative tissues was investigated. Furthermore, a cell death phenotype was observed in transgenic *B. distachyon* following ectopic expression of *WRI1*, suggesting that cytotoxic effects of free FAs might be the cause.

RESULTS

Overexpression of *BdWRI1* Increases Grain TAG Content in *B. distachyon*

To identify possible WRI1 orthologs in *B. distachyon*, a BLASTP analysis was performed with an e-value threshold of 1.0E-10 in Phytozome (http://www.phytozome.net/). The Arabidopsis WRI1 sequence was used in a query against the *B. distachyon* protein database, and 24 AP2 domain-containing proteins were identified. Phylogenetic analysis by MEGA6 (Tamura et al., 2013) showed that the protein encoded by *Bradi4g43877* was the closest ortholog to AtWRI1 (Fig. 1). We tentatively designated *Bradi4g43877* as *BdWRI1*. Further alignment of AtWRI1 and BdWRI1 revealed that these two proteins share 76% sequence identity over 420 amino acids covering the full length of BdWRI1. In

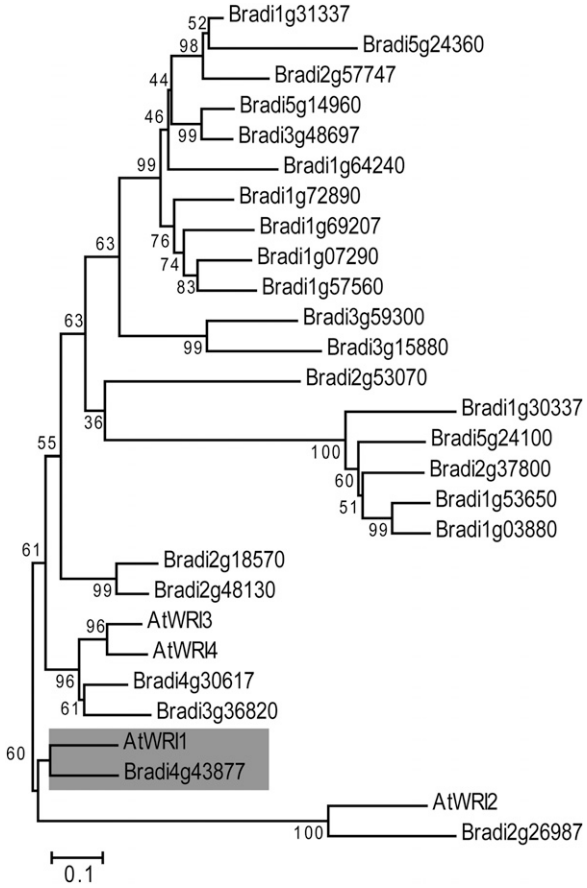

Figure 1. Phylogenetic tree of Arabidopsis WRI1 homologs and presumed *B. distachyon* AP2 domain-containing WRI1 orthologs. A neighbor-joining tree was generated using all full-length *B. distachyon* AP2 domain-containing protein sequences that are presumed orthologs of the WRI1 proteins from Arabidopsis. The sequences were aligned with ClustalW. An unrooted phylogenetic tree was constructed with MEGA6 using the neighbor-joining method, and the bootstrap values were derived from 1,000 replicates. The gray box indicates AtWRI1 and its presumed ortholog in *B. distachyon*.

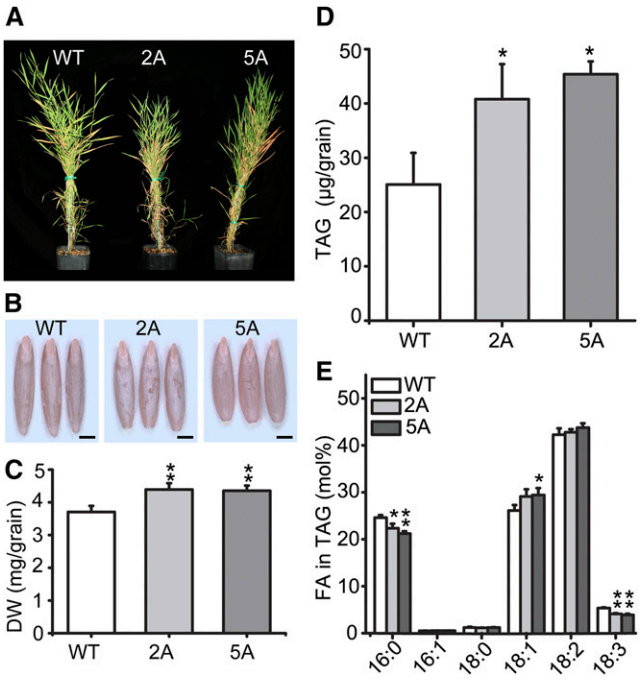

Figure 2. Overexpression of *BdWRI1* increases grain TAG content. A, Phenotypes of 15-week-old *UBI*::*BdWRI1* plants. B, Phenotypes of *UBI*::*BdWRI1* grains without lemma. Bars = 1 mm. C, Dry weights (DW) of *UBI*::*BdWRI1* grains. Each sample contained 15 grains. Data represent three independent measurements, and the error bars represent SD. Asterisks indicate significant differences by Student's *t* test: **, $P \leq 0.01$. D and E, TAG contents (D) and FA composition of TAG (E) from dry grains of *UBI*::*BdWRI1* and Bd21-3. Total lipids were extracted from the grains. Each sample contained five grains. Three independent measurements were averaged, and the error bars represent SD. Asterisks indicate significant differences by Student's *t* test: *, $P < 0.05$; and **, $P \leq 0.01$. WT, Wild type.

addition, the sequence VYL present in the first AP2 domain of AtWRI1, which is essential for its function (Ma et al., 2013), was also conserved in BdWRI1 (Supplemental Fig. S1).

To obtain in planta experimental verification that BdWRI1 is a true ortholog, we overexpressed *BdWRI1* in *B. distachyon* under the control of the maize ubiquitin promoter (*ZmUBI1*). Ten independent transgenic *B. distachyon* lines were generated that harbored the *BdWRI1* overexpression construct. Two lines (2A and 5A; Fig. 2A) were found to have high ectopic *WRI1* expression relative to wild-type Bd21-3 and were selected for further analysis.

Since *AtWRI1* overexpression affects seeds of Arabidopsis (Cernac and Benning, 2004), we tested whether the overexpression of *BdWRI1* could influence grain development and TAG accumulation in *B. distachyon*. The grain dry weights were increased approximately 20% compared with Bd21-3 (Fig. 2, B and C). To further determine the effect of BdWRI1 on storage oil accumulation, total lipid was extracted from dry grains and FA methylesters were analyzed by gas chromatography. The *UBI*::*WRI1* lines 2A and 5A showed considerably higher TAG content, 60% and 80% higher (40.8 ± 6.5 and 45.4 ± 2.4 μg grain^{-1}), respectively, compared with wild-type Bd21-3 (25.1 ± 5.8 μg grain^{-1}; Fig. 2D). The acyl group profiles of grain TAGs changed slightly, but statistically significantly, with slight decreases in 16:0 (carbon:double bonds) and 18:3 and an increase in 18:1 (Fig. 2E).

To determine the tissue of grains in which TAG is sequestered into lipid droplets, dry grains of Bd21-3, together with the *UBI*::*BdWRI* 2A and 5A lines, were stained with Nile Red and observed by confocal microscopy. In Arabidopsis, most of the storage TAGs accumulate in the embryo, whereas endosperm stores only 10% of the seed TAG (Penfield et al., 2004; Miquel et al., 2014). However, in *B. distachyon* Bd21-3 grains, most of the storage lipid apparently accumulates in the endosperm, indicated by the presence of lipid droplets (Fig. 3, D–F), while no obvious lipid droplets were observed in the embryo (Fig. 3, A–C). Similar to oat grains (Heneen et al., 2008), most of the lipid droplets in the starchy endosperm were fused with each other, forming a continuous lipid matrix between the protein and starch components. Only a few discrete lipid droplets were observed in the endosperm (Fig. 3, D–F). In contrast, the number of lipid droplets was higher in the endosperm of *UBI*::*BdWRI1* line 2A (Fig. 3, J–L) and line 5A (Supplemental Fig. S2, D–F) compared with the wild type (lipid droplets per cell of 10 cells examined: wild

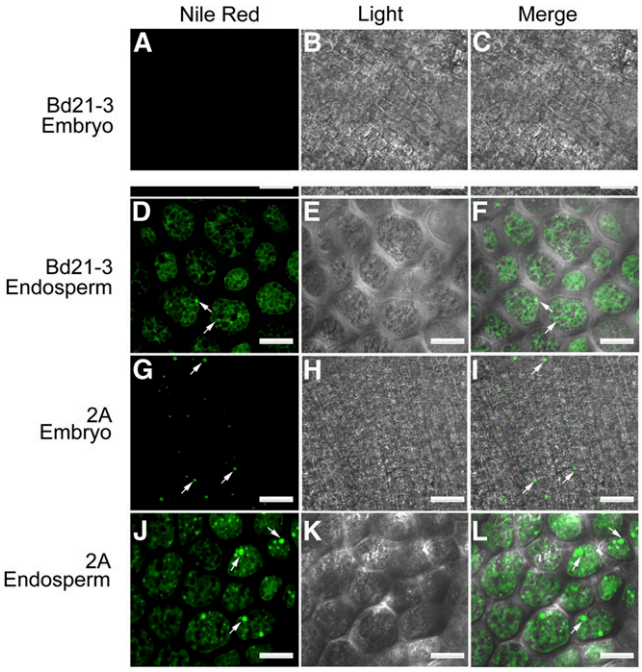

Figure 3. Lipid droplets are abundant in embryo and endosperm of *UBI*::*BdWRI1* dry grains. A to F, Confocal fluorescence images of dry grains of Bd21-3 showing few lipid droplets (arrows) in the endosperm. G to L, Confocal fluorescence micrographs of dry grains of *UBI*::*BdWRI1* line 2A. Lipid droplets were observed in both embryo and endosperm. Bars = 20 μm.

type, 2.5 ± 1; 2A, 4.1 ± 1; and 5A, 7.6 ± 2.8), but lipid droplet size was not statistically different. Taken together, similar to AtWRI1 (Cernac and Benning, 2004; Cernac et al., 2006), BdWRI1 also seems to affect TAG biosynthesis in storage tissues, in the case of *B. distachyon* in the embryo and endosperm.

Ectopic Expression of *BdWRI1* Leads to TAG Accumulation in Leaf Blades

To explore whether the presence of BdWRI1 in vegetative tissues enhances TAG accumulation, the abundance of *BdWRI1* mRNA in the transgenic leaf blades was determined by quantitative real-time (RT)-PCR using *UBIQUITIN-CONJUGATING ENZYME18* (*BdUBC18*, *Bradi4g00660*) as an internal control (Hong et al., 2008). In the *UBI*::*WRI1* lines, transcription levels of *WRI1* in 8-week-old plants were 552- and 380-fold higher than in Bd21-3 (Fig. 4A). To test whether BdWRI1 affects the metabolism required for FA biosynthesis in vegetative tissues, presumed orthologs of known WRI1 target genes in dicotyledonous plants (Maeo et al., 2009), such as *PLASTIDIC PYRUVATE KINASE β-SUBUNIT1* (*PKPβ1*), *ACYL-CARRIER PROTEIN1* (*ACP1*), and *KETOACYL-ACYL-CARRIER PROTEIN SYNTHASE I* (*KASI*), were identified in the *B. distachyon* protein database. When normalized to Bd21-3, the mRNA levels of *PKPβ1* (*Bradi2g45620*) and *BdACP1* (*Bradi1g01000*) were enhanced 74- and 51-fold, respectively, whereas *BdKASI* (*Bradi1g46610*) expression increased 6.2-fold (Fig. 4B). Taken together, ectopic expression of *BdWRI1* led to the induction of presumed orthologs of genes involved in FA biosynthesis in *B. distachyon* leaf blades.

In addition, TAG content in 8-week-old leaf blades was increased. As shown in Figure 4C, TAG levels in transgenic lines 2A and 5A were 32.5- and 30-fold higher (1.3 ± 0.4 and 1.2 ± 0.1 $\mu g\ mg^{-1}$ dry weight) than in Bd21-3 (0.04 ± 0.01 $\mu g\ mg^{-1}$ dry weight). The ectopic expression of *BdWRI1* also resulted in an increase in polyunsaturated FAs at the expense of saturated FAs in TAGs (Fig. 4D), which could be derived from membrane lipids that are being turned over.

It should also be noted that an increased number of lipid droplets was observed in stem internodes of *UBI*::*BdWRI1* transgenic *B. distachyon* (Supplemental Fig. S3), suggesting that TAG accumulation is stimulated in different vegetative tissues of the transgenic plants.

Ectopic Expression of *BdWRI1* in *B. distachyon* Causes Cell Death in Leaf Blades

In addition to TAG accumulation, browning of leaf blades due to premature cell death was observed in the vegetative tissues of *UBI*::*WRI1* transgenic plants. Leaf necrotic lesions were first visible in 4-week-old transgenic lines and expanded rapidly during development, whereas Bd21-3 leaves remained green and healthy looking (Fig. 5A). A first sign of the readily ascertainable

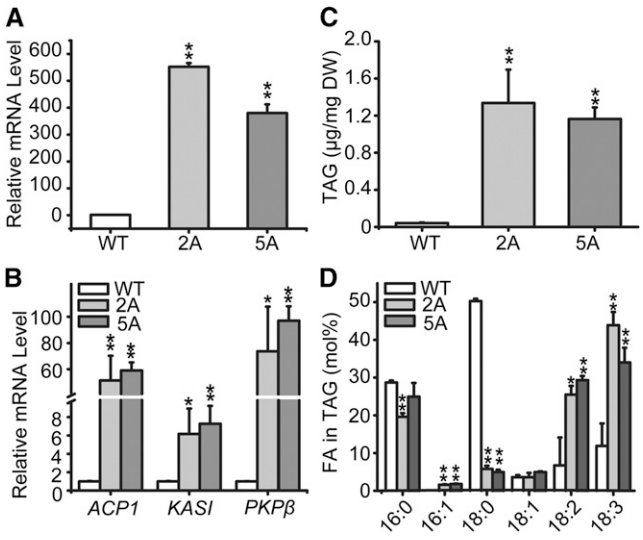

Figure 4. Ectopic expression of *BdWRI1* increases TAG content in *B. distachyon* leaf blades. A and B, Expression levels of *BdWRI1* (A) glycolysis and FA biosynthesis orthologs (B) in 8-week-old leaf blades. Total RNA was isolated, and relative mRNA levels were determined by quantitative RT-PCR using *BdUBC18* as an internal control. Three independent measurements were averaged, and the error bars represent SD. Asterisks indicate significant differences by Student's *t* test: *, $P < 0.05$; and **, $P \leq 0.01$. C and D, TAG contents (C) and FA composition of TAG (D) of 8-week-old leaf blades. Total lipids were extracted, and TAG was separated by thin-layer chromatography (TLC). Three independent measurements were averaged, and the error bars represent SD. Asterisks indicate significant differences by Student's *t* test: *, $P < 0.05$; and **, $P \leq 0.01$. DW, Dry weight; WT, wild type.

consequence of cell death in plant tissue is increased membrane permeability measured by increased electrolyte leakage, which can be used to quantify cell death (Baker and Orlandi, 1995; Dellagi et al., 1998; Torres et al., 2002; Hofius et al., 2009). Measurement of percentage of electrolyte leakage in 8-week-old detached leaves was up to 9.3-fold increased in *UBI*::*BdWRI1* leave blades (Fig. 5B). It should be mentioned that constitutive expression of *AtWRI1* in *B. distachyon* under the control of the *ZmUBI1* promoter also led to brown lesions and reactive oxygen species (ROS) accumulation (Supplemental Fig. S4), which suggests that cell death in *UBI*::*BdWRI1* plants is caused by the species context rather than by functional differences between AtWRI1 and BdWRI1. However, it should be noted that ectopic expression of *AtWRI1* in Arabidopsis did not cause visible cell death or electrolyte leakage under comparable conditions (Supplemental Fig. S5).

ROS including hydrogen peroxide (H_2O_2), superoxide, singlet oxygen, and hydroxyl radicals have been closely associated with plant cell death (del Rio et al., 1998; Apel and Hirt, 2004; Danon et al., 2005; Schmitt et al., 2014). ROS not only cause oxidative damage to cellular constituents, they also act as signals that play a crucial role in the activation of processes leading to cell death (Apel and Hirt, 2004; Baxter et al., 2014; Schmitt et al., 2014). To test if ROS accumulate in *UBI*::*BdWRI1*

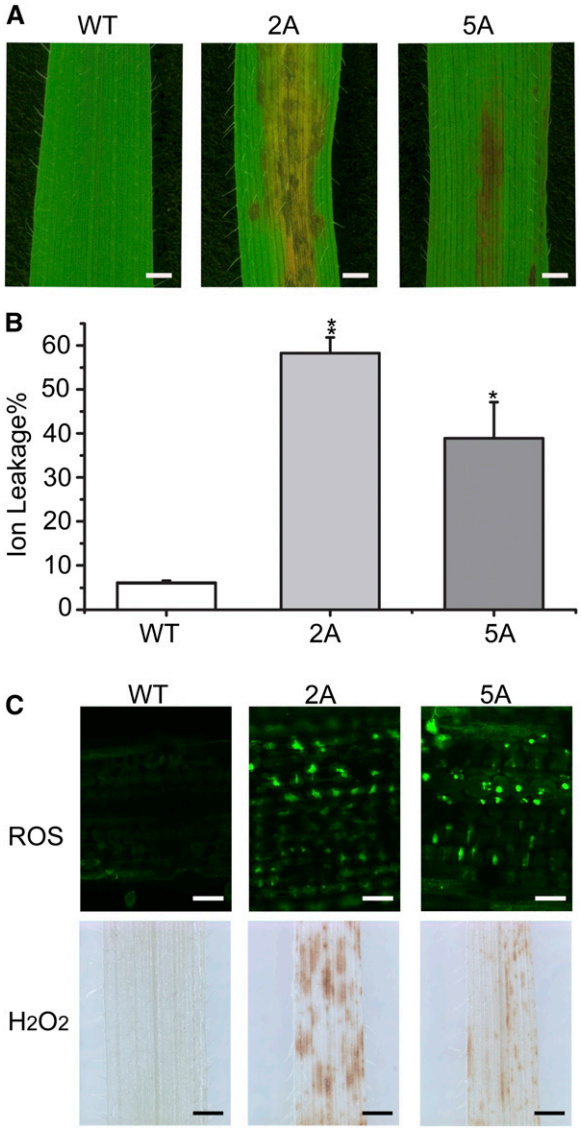

Figure 5. Premature cell death in the leaf blades of *UBI*::*BdWRI1* lines. A, Phenotypes of 8-week-old *UBI*::*BdWRI1* leaf blades. Bars = 1.25 mm. B, Quantification of cell death by electrolyte leakage assay. Eight-week-old detached leaf blades were inoculated with water for 3 h, and then the conductivity of the water was measured. Each value represents the mean and SD of three replicates per experiment. Asterisks indicate significant differences by Student's *t* test: *, $P < 0.05$; and **, $P \leq 0.01$. C, ROS accumulation in 8-week-old leaf blades of *UBI*::*BdWRI1* lines and the wild type (WT). General ROS accumulation was detected by H_2DCF-DA staining (top; bars = 20 μm), and H_2O_2 accumulation was detected by DAB staining (bottom; bars = 1 mm).

leaves, 2′,7′-dichlorofluorescein diacetate acetyl ester (H_2DCF-DA) was used as an indicator (Schmitt et al., 2014). ROS-dependent fluorescence of H_2DCF-DA in leaf tissues was measurably stronger in *UBI*::*BdWRI1* lines (Fig. 5C, top). In addition, 3-diaminobenzidine (DAB) was used as an indicator of H_2O_2 accumulation (Fryer et al., 2002; Ramel et al., 2009; Schmitt et al., 2014). Widespread DAB staining was seen in *UBI*::*BdWRI1* leaves even in the areas that did not yet have brown lesions (Fig. 5C, bottom). Taken together, the ectopic expression of *BdWRI1* causes cell death in the leaf tissues of *B. distachyon*, which is likely preceded by an increase in ROS.

Free FAs Increased following *BdWRI1* Ectopic Expression

In all previously reported cases of ectopic expression of *WRI1* to induce the accumulation of TAG in vegetative tissues (Cernac and Benning, 2004; Sanjaya et al., 2011; Vanhercke et al., 2013, 2014), cell death has never been observed. These studies were all done with dicotyledonous plants. Thus, we focused on determining the possible mechanisms of cell death in *UBI*::*BdWRI1* lines, as this might reveal differences in lipid metabolism and regulation between dicotyledonous and monocotyledonous plants. The accumulation of free FAs is known to have cytotoxic effects not only in yeast and mammalian cells (Garbarino et al., 2009; Kohlwein, 2010; Lee et al., 2010; Fakas et al., 2011) but also in microalgae and plants (Wu et al., 2006; Bosma et al., 2008; Fan et al., 2013, 2014). Since the expression of several presumed orthologs of genes involved in FA biosynthesis was highly induced in *UBI*::*BdWRI1* plants (Fig. 4B), possibly resulting in increased free FA levels, we asked whether the accumulation of free FAs was a factor in the observed induction of cell death. As shown in Figure 6A, free FA contents in 8-week-old leaf blades of *UBI*::*BdWRI1* plants were up to 2-fold increased. In contrast, ectopic expression of *AtWRI1* in Arabidopsis did not lead to substantial changes in free FAs (Supplemental Fig. S6B), indicating that free FAs might be the cause of species-specific cell death in *B. distachyon* ectopically expressing *WRI1*.

The majority of the free FAs in *UBI*::*BdWRI1* leaves were found to be 16:0, 18:2, and 18:3 (Fig. 6B), which corresponded to the FA composition of leaf TAG (Fig. 4D). Therefore, we reasoned that free FAs might be derived from TAG turnover. To examine the origin of free FAs in these lines, the expression of possible orthologs encoding enzymes involved in the degradation of TAGs was analyzed by RT-PCR. Arabidopsis *SDP1* encodes a TAG lipase that catalyzes the initial step in TAG breakdown (Eastmond, 2006; Padham et al., 2007), while the β-oxidation pathway subsequently breaks down the released FAs (Goepfert and Poirier, 2007). As shown in Figure 6C, both presumed orthologs of *SDP1* (*BdSDP1-1* [*Bradi2g50610*] and *BdSDP1-2* [*Bradi1g04310*]) and presumed β-oxidation pathway genes, such as *ACYL-CoA OXIDASE1* (*ACX1*; *Bradi1g52320*), *ACX2* (*Bradi4g14090*), *KETOACYL-CoA THIOLASE1* (*KAT1*; *Bradi3g27960*), *KAT2* (*Bradi3g55420*), *LONG-CHAIN ACYL-CoA SYNTHEASE6* (*LACS6*; *Bradi4g26610*), *LACS7* (*Bradi4g42950*), and *MULTIFUNCTIONAL PROTEIN2* (*MFP2*; *BdMFP2-1* [*Bradi2g43020*], *BdMFP2-2* [*Bradi4g28310*], and *BdMFP2-3* [*Bradi4g28310*]), were induced, indicating that ectopic expression of *BdWRI1* also might cause accelerated TAG turnover. As H_2O_2 is a by-product of β-oxidation (Graham and Eastmond, 2002; Eastmond, 2007), the observed induction of the β-oxidation

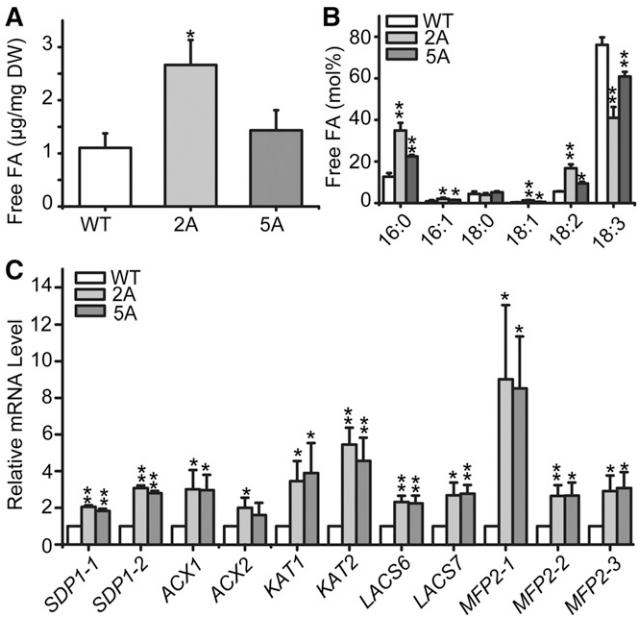

Figure 6. Elevated free FA levels in *UBI*::*BdWRI1* leaf blades. A and B, Free FA contents (A) and FA composition (B) in 8-week-old leaf blades. Total lipids were extracted, and free FAs were separated by TLC. Three independent measurements were averaged, and the error bars represent SD. Asterisks indicate significant differences by Student's *t* test: *, $P < 0.05$; and **, $P \leq 0.01$. C, Expression of genes predicted to encode proteins involved in TAG degradation in 8-week-old leaf blades. Total RNA was isolated, and relative mRNA levels were determined by quantitative RT-PCR using *BdUBC18* as an internal control. Three independent measurements were averaged, and the error bars represent SD. Asterisks indicate significant differences by Student's *t* test: *, $P < 0.05$; and **, $P \leq 0.01$. DW, Dry weight; WT, wild type.

pathway raises the possibility that the accumulation of H_2O_2 in *UBI*::*BdWRI1* plants may partially be caused by increased TAG turnover.

Application of Free FAs to *B. distachyon* Leaf Blades Leads to Cell Death

To test whether increased free FAs could be linked to cell death in *UBI*::*BdWRI1* plants, we examined the effects of free FA application to leaves of Bd21-3. Because in *UBI*::*BdWRI1* plants 18:2 and 16:0 were the most increased free FAs (Fig. 6B), 3-week-old detached Bd21-3 leaf blades were inoculated with 200 μM 18:2. After 48 h of treatment, brown lesions were observed (Fig. 7A), which resembled those present in *UBI*::*BdWRI1* plants (Fig. 5A). In addition, externally applied 16:0 also caused brown lesions in Bd21-3 leaves (Supplemental Fig. S7). But because of the low solubility of 16:0, 18:2 was chosen for the following experiments.

To further investigate the influence of free FAs on cell death, 3-week-old Bd2-3 leaves were treated with 0, 50, 100, or 200 μM 18:2. Electrolyte leakage was monitored throughout a 48-h period. As shown in Figure 7B, the 18:2-treated leaves showed increases in electrolyte leakage, which were highest at 200 μM at every time point. Therefore, *B. distachyon* is sensitive to 18:2 at low concentrations and in a time-dependent manner.

Inhibition of FA Biosynthesis Decreases 18:2-Induced Cell Death in Leaf Blades

Because WRI1 directly activates genes encoding proteins involved in FA synthesis (Baud et al., 2009; Maeo et al., 2009) and ectopic expression of *BdWRI1* induced free FA accumulation, appearing to cause premature cell death in vegetative tissues, we postulated that an inhibition of FA biosynthesis in *UBI*::*BdWRI1* plants might reduce free FA levels in vivo, thus ameliorating the observed cell death. To test this hypothesis, detached 3-week-old leaf blades not yet showing lesions in the transgenic lines were treated with 200 μM 18:2 in the presence or absence of 5 μM cerulenin, a specific inhibitor of KAS I and KAS II, which are key enzymes of de novo FA biosynthesis (Awaya et al., 1975; Packter and Stumpf, 1975; Koo et al., 2005). The extent of cell death was evaluated by electrolyte leakage measurements.

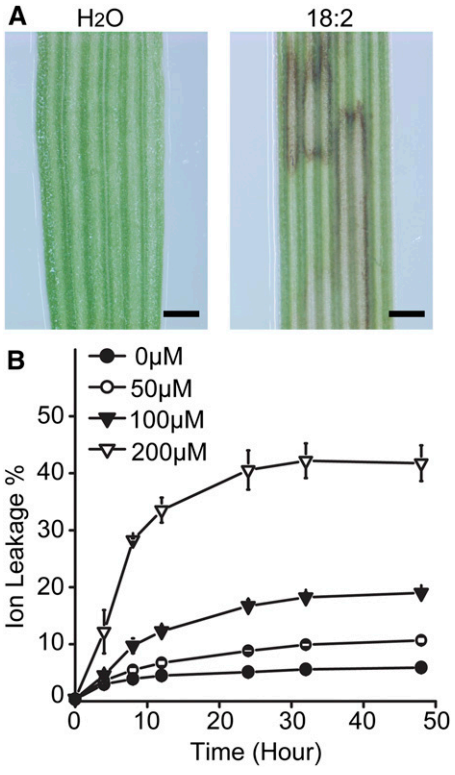

Figure 7. 18:2 Treatment causes cell death in *B. distachyon* leaf blades. A, Phenotypes of wild-type Bd21-3 detached leaf blades treated with 200 μM 18:2 for 48 h. Bars = 0.5 mm. B, Quantification of electrolyte leakage as an indicator for cell death during 18:2 treatment. Three-week-old detached leaf blades were inoculated with water containing different concentrations of 18:2, and conductivity changes were measured at different time points. Each value represents the mean and SD of three replicates per experiment.

During all the treatments without 18:2, ion leakage stayed at a low level during 48 h. When 200 μM 18:2 was added to either *UBI*::*BdWRI1* plants or Bd21-3, the ion leakage increased, whereas the addition of 5 μM cerulenin strongly inhibited 18:2-induced cell death (Fig. 8), which demonstrated that premature cell death in leaf blades of *UBI*::*BdWRI* was at least partially caused by increased free FAs.

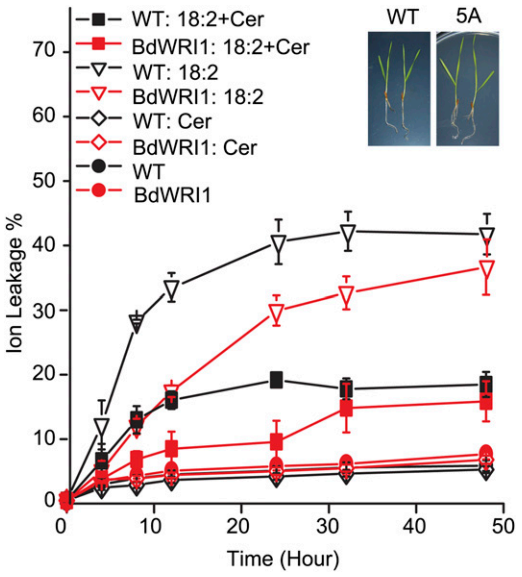

Figure 8. Cerulenin strongly inhibits 18:2-induced electrolyte leakage as an indicator for cell death in *B. distachyon* leaf blades. Detached 3-week-old leaf blades were inoculated with water containing 200 μM 18:2 and 5 μM cerulenin (Cer) for 48 h. Conductivity changes were measured at different time points. Each value represents the mean and SD of three replicates per experiment. Three-week-old Bd21-3 and *UBI*::*BdWRI1* seedlings not yet showing the cell death phenotype are shown in the insets. WT, Wild type.

DISCUSSION

WRI1 Has a Conserved Function in FA Biosynthesis and TAG Accumulation

In the Arabidopsis *wri1* mutant, TAG contents in embryo and endosperm were reduced (Cernac et al., 2006). Conversely, we found that the number of lipid droplets was higher in embryo and endosperm of *UBI*::*BdWRI1* expressing *B. distachyon* (Fig. 3; Supplemental Fig. S2). Thus, WRI1 has a conserved function during storage TAG accumulation in seed tissues. It should also be noted that the structural features of lipid droplets in the *B. distachyon* endosperm changed when *BdWRI1* was overexpressed. Most of the lipid droplets tended to fuse with each other in Bd21-3 (Fig. 3, D–F). In contrast, more discrete lipid droplets were observed in the *UBI*::*BdWRI1* lines (Fig. 3, J–L; Supplemental Fig. S2, D–F). Coalescence of the lipid droplets has also been observed in oat endosperm (Heneen et al., 2008), probably related to the amount of lipid droplet-associated proteins, such as OLEOSIN, present in the tissue.

Furthermore, in addition to the increased TAG content in leaf blades, ectopic expression of *BdWRI1* also increased the number and size of lipid droplets in stem internodes (Supplemental Fig. S3), suggesting that this approach enhances TAG accumulation in all vegetative tissues of *B. distachyon*. These results are consistent with previous studies conducted in dicotyledonous plants (Cernac and Benning, 2004; Sanjaya et al., 2011; Dussert et al., 2013; Kelly et al., 2013; Vanhercke et al., 2013, 2014; Grimberg et al., 2015) and confirm that BdWRI1 has a conserved function in regulating FA and, indirectly, TAG biosynthesis and that ectopic production of WRI1 serves as a promising tool for enhancing the energy density in vegetative tissues of plants.

Although TAG content increased in both storage and vegetative tissues of *UBI*::*BdWRI1* plants, the FA composition of TAGs in these tissues differed notably. In grain TAGs, approximately 30% of the FAs were de novo synthesized 18:1, whereas 18:3 was less than 6% (Fig. 2E). In striking contrast, the most abundant FA in leaf TAG was 18:3 (nearly 45% of the FAs in TAG), while 18:1 made up only 4% (Fig. 4D). Plants can use alternative routes to produce TAGs: first, TAG assembly from newly synthesized FAs by the Kennedy pathway, which generates TAGs rich in 18:1; and second, from intermediates such as phosphatidylcholine (PtdCho) subjected to acyl-chain editing, which provides polyunsaturated FAs or diacylglycerol rich in polyunsaturated FAs for TAG assembly (Bates and Browse, 2011, 2012; Bates et al., 2012, 2013). Relative fluxes through these pathways vary widely depending on plant species, tissues, and developmental stages (Bates and Browse, 2012), and they are still unclear for *B. distachyon*. However, the current results provide evidence that, in *B. distachyon*, TAG synthesis in storage tissues may rely more on the Kennedy pathway, while vegetative tissues may be more dependent on acyl editing and PtdCho-derived precursors to produce polyunsaturated FA-containing TAGs.

Functional Divergence of Lipid Metabolism between Monocots and Dicots

Much of our current understanding of plant gene function is based on the dicotyledonous model plant Arabidopsis. Although many proteins show conserved sequences in different plant species, even highly similar proteins can play distinct, although related, roles in a species-specific context. For instance, while grasses and dicotyledonous plants share many orthologs determining inflorescence development, the corresponding grass orthologs display variations in copy numbers, distinct expression patterns, and functional complexity, which are likely associated with the distinct inflorescence morphogenesis in grasses (Zhang and Yuan, 2014). For example, in the blue light signaling pathway, the interaction between CRYPTOCHROME-INTERACTING basic Helix-Loop-Helix1 (CIB) and CRYPTOCHROME (CRY)

is evolutionarily conserved. However, the primary function of the CRY2-CIB complex in Arabidopsis is the regulation of flowering time, whereas the regulation of leaf senescence appears to be the major physiological function in soybean (*Glycine max*; Meng et al., 2013).

Functional divergence between monocotyledonous and dicotyledonous plants is also prominent in plant storage lipid metabolism. For example, oilseed plants such as Arabidopsis and some *Brassica* spp. have evolved to accumulate large amounts of TAG as energy stores in embryonic tissues, whereas *B. distachyon* and other Poaceae accumulate large amounts of polysaccharides in endosperm tissues instead (Penfield et al., 2004; Guillon et al., 2012). Despite the fact that WRI1 shows conserved function in FA biosynthesis and oil production in planta, different expression patterns of *WRI1* orthologs or additional phenotypes of the respective overexpression or mutant lines have been reported in many species. *AtWRI1* is specifically expressed in siliques, whereas oil palm *EgWRI1* is highly expressed in mesocarp (Tranbarger et al., 2011; Dussert et al., 2013). The Arabidopsis *wri1* mutant does not show any obvious phenotype in nonseed tissues (Focks and Benning, 1998), whereas silencing of *WRI1* expression in cotton (*Gossypium* spp.) resulted in increased fiber length (Qu et al., 2012). Here, we observed that ectopic expression of *BdWRI1* caused cell death in *B. distachyon* (Fig. 5), which is not observed for Arabidopsis (Supplemental Fig. S5).

Taken together, these findings argue that WRI1-dependent regulation of carbon flow from sugars to FAs is an evolutionarily conserved mechanism in plants, while the specific phenotypes of ectopic expression depend on species context.

TAG Turnover Is Increased in Vegetative Tissues of *B. distachyon*

During the course of this work, we specifically tried to address the species differences between *B. distachyon* and Arabidopsis leading to cell death only in *B. distachyon* when *WRI1* is ectopically expressed. Since free FAs could be the causal link to the cell death phenotype, the metabolic origin of the free FAs in *UBI*::*BdWRI1* plants may provide the necessary insight. The free FAs accumulating in *B. distachyon* transgenic plants may derive from at least three possible sources: (1) de novo synthesized FAs that directly enter the free FA pool; (2) recycled FAs derived from PtdCho acyl editing; and (3) free FAs that arise from the enhanced turnover of leaf TAG.

In *UBI*::*BdWRI1* leaf blades, the FA composition of TAG and free FAs was similar, as both contained more than 60% of polyunsaturated FAs, while 18:1 was present at less than 5% (Figs. 4D and 6B), which indicates that most of the free FAs are unlikely from the de novo synthesized FA pool. PtdCho is a major substrate for FA desaturation, and acyl editing of PtdCho is an integral component of eukaryotic glycerolipid synthesis (Bates et al., 2007). Therefore, increased amounts of polyunsaturated free FAs may indicate that the formation of FAs by PtdCho acyl editing is faster than FA utilization for TAG and membrane lipid synthesis.

In addition, extensive experimental evidence indicates that free FAs supplied to tissues are sequestered into TAGs (Roughan et al., 1987; Koo et al., 2005; Tjellström et al., 2015). These TAGs undergo substantial and rapid turnover (Tjellström et al., 2015). Moreover, the expression of many orthologs presumed to encode enzymes involved in TAG degradation was induced, suggesting that this pathway is highly active (Fig. 6C) in *UBI*::*BdWRI* plants. In contrast, the composition of free FAs (Supplemental Fig. S6C) and TAG (Supplemental Fig. S6D) was strikingly different, and the TAG degradation pathway was not induced (Supplemental Fig. S6E) in *35S*::*AtWRI1* Arabidopsis plants. Based on these data and considerations, leaf TAG turnover appears to occur more rapidly in *B. distachyon* than in Arabidopsis, resulting in the observed increase in free FAs in *UBI*::*BdWRI* leaf blades.

Indirect support for the contribution of TAG turnover to the free FA pool was obtained by a delayed effect of 18:2 application-induced cell death in *UBI*::*BdWRI1*-expressing *B. distachyon* leaves (Fig. 8). Because TAG in vegetative tissues can serve as a buffer for FAs and, thereby, protect against free FA-induced cell death (Kunz et al., 2009; Fan et al., 2013), increased TAG accumulation in *UBI*::*BdWRI1* vegetative tissues may enhance the TAG-buffering capacity, allowing the intermittent sequestration of applied 18:2. Alternatively, we cannot rule out that the delayed cell death in *UBI*::*BdWRI1* lines may be caused by the sequestration of FAs in other structures such as the epidermis or that there may be an adaptive response to sublethal levels of 18:2.

Mammalian cells have at least two mechanisms to prevent free FA-induced cell death: (1) inhibition of FA synthesis; and (2) sequestration of excess free FAs into TAGs in lipid droplets (Lee et al., 2010). Similar mechanisms exist in plants. For instance, feedback inhibition of FA biosynthesis has been demonstrated in various plant systems (Terzaghi, 1986; Shintani and Ohlrogge, 1995; Andre et al., 2012). Additionally, changing the TAG accumulation in plant cells can influence the sensitivity to free FA-induced cell death. PDAT1 is reported to play a role in TAG biosynthesis and lipid homeostasis in Arabidopsis leaves (Fan et al., 2013, 2014); an Arabidopsis *pdat1 trigalactosyldiacylglycerol1* (*tgd1*) double mutant showed reduced leaf TAG content compared with a *tgd1* single mutant and displayed a hypersensitive response to free FAs (Fan et al., 2013). Here, we demonstrate an opposite scenario. Although it has been shown that WRI1 is not directly involved in the transcriptional control of genes encoding the final enzymes of TAG synthesis (Baud et al., 2009; Maeo et al., 2009), TAG content increased in *UBI*::*BdWRI1* lines (Fig. 4C). This increased TAG content may have led to an enhanced protective capacity for free FAs

applied to the transgenic plants, leading to a delayed cell death (Fig. 8). These results are consistent with the notion that TAG pools play an important role in detoxifying free FAs also in plants.

CONCLUSION

Increasing energy density in plant biomass by increasing the TAG content is synergistic with efforts to develop lignocellulosic feedstock for biofuel production. Producing only 10% of TAG (by dry weight) in vegetative tissues will increase the energy yield approximately 40% in biomass crops compared with fermentation to ethanol alone (Ohlrogge and Chapman, 2011). Thus, the accumulation of TAGs in the vegetative tissues of biomass crops is a promising strategy. Although ectopic expression of *BdWRI1* induced TAG accumulation in vegetative tissues of *B. distachyon*, cell death was also observed. Second-generation transgenic *B. distachyon* plants have to encompass tissue-specific or inducible expression of *WRI1* to avoid these deleterious effects. Because TAGs seem to be rapidly turned over in *B. distachyon* leaf blades, inhibition of TAG degradation along with ectopic expression of *WRI1* might provide a more viable strategy to enhance the energy density in monocotyledonous plants.

MATERIALS AND METHODS

Plant Materials and Growth Conditions

Arabidopsis (*Arabidopsis thaliana*) Columbia-2 and *35S::AtWRI1* seeds (Sanjaya et al., 2011) were sterilized and plated on Murashige and Skoog medium (Murashige and Skoog, 1962) containing 1% (w/v) Suc. After 7 d, the seedlings were transferred to soil containing 22 $\mu g\ g^{-1}$ nitrate, 3.8 $\mu g\ g^{-1}$ phosphorus, 63 $\mu g\ g^{-1}$ potassium, 75 $\mu g\ g^{-1}$ calcium, 57 $\mu g\ g^{-1}$ magnesium, 34 $\mu g\ g^{-1}$ sodium, and 16 $\mu g\ g^{-1}$ chloride. Seeds were kept at 4°C for 72 h in the dark and then grown in 100 to 200 $\mu E\ m^{-2}\ s^{-1}$ with a 16-h-light/8-h-dark cycle and 22°C/18°C (day/night). *Brachypodium distachyon* Bd21-3 and *UBI::BdWRI1* grains were wet briefly with 70% (v/v) ethanol and then surface sterilized with 10% (v/v) bleach containing 0.01% (v/v) SDS for 5 min. Grains were rinsed thoroughly with sterile water five times. The surface-sterilized grains were placed onto Murashige and Skoog medium without Suc. After 7 d, the seedlings were transferred to the same soil mentioned above. Plants were grown under 150 $\mu E\ m^{-2}\ s^{-1}$ with a 16-h-light/8-h-dark cycle and 22°C/18°C (day/night).

Plasmid Construction and *B. distachyon* Transformation

Total RNA was isolated from 44-d-old Bd21-3 flowers using the Plant RNeasy RNA extraction kit (Qiagen), and then 0.5 μg of RNA was reverse transcribed using *Moloney murine Leukemia Virus* Reverse Transcriptase (Promega) and oligo$(dT)_{18}$ following the manufacturers' protocols. A *BdWRI1* (Bradi4g43877) overexpression construct was built by amplifying a 1.27-kb full-length complementary DNA sequence using forward 5′-GGGGGTACCCATGAAGAGATCCCCTCCTCAGCCGTC-3′ and reverse 5′-GGGGAATTCTCAATTGCACACAGTGATCATTTTTGG-3′ primers and inserting it using restriction enzymes into pENTR2B (Thermo Fisher). These entry clones are recombined into the plant expression vector pIPKb002 (Himmelbach et al., 2007) using LR clonase (Thermo Fisher). Entry and expression clones were verified by sequencing. Transgenic *B. distachyon* plants harboring the *BdWRI1* overexpression construct were regenerated from *Agrobacterium tumefaciens*-mediated transformed Bd21-3 embryonic callus tissue (Vogel and Hill, 2008) using *A. tumefaciens* strain AGL-1 and medium supplemented with 40 units mL^{-1} hygromycin B (Phytotechnology Laboratories).

Lipid Analysis

TAG and free FA analyses were performed as described previously but with minor modifications (Sanjaya et al., 2013). *B. distachyon* or Arabidopsis leaf tissues were harvested and freeze dried. Total lipids were extracted from approximately 20 mg of dry tissues or five dry grains with lipid extraction buffer (chloroform:methanol:formic acid, 10:20:1, v/v), with 10 μg of tri-17:0 TAG (Sigma) and 10 μg of 15:0 (Sigma) added as internal standards. Total lipid samples were separated by TLC on silica plates (Si250PA; Mallinckrodt Baker) developed with ether:ethyl ether:acetic acid (80:20:1, v/v). After development, TAG and free FA bands were sprayed with 0.01% (v/v) Primuline in 80% (v/v) acetone and visualized under UV light. TAG or free FA bands were isolated from the TLC plate. FA methyl esters were prepared and quantified as described (Wang and Benning, 2011).

Quantitative Real-Time PCR

Total RNA from 4-week-old Arabidopsis leaves or 8-week-old *B. distachyon* leaf blades was isolated using an RNeasy Plant Mini Kit (Qiagen). One microgram of total RNA was used to synthesize complementary DNA using SuperScript III Reverse Transcriptase (Invitrogen). Quantitative RT-PCR was performed using the SYBR Green PCR Core Reagents mix (Thermo Fisher) following the manufacturer's manual. Supplemental Table S1 lists the primers used in this research. The $2^{-\Delta\Delta Ct}$ calculation as described in (Livak and Schmittgen, 2001) was used to determine the relative mRNA levels.

Electrolyte Leakage Assay

Electrolyte leakage assays were performed as described (Gilmour et al., 1988), but with minor modifications. Three to four 3-week-old detached *B. distachyon* leaf blades were immersed in 5 mL of deionized water, and the samples were gently agitated for 3 h. Conductivity was measured using a conductance meter (YSI model 35). One hundred percent leakage was obtained by placing the leaves in −80°C for 1 h. Electrolyte leakage was expressed as a percentage of the final ion leakage.

Microscopy

Lipid droplets were observed using Nile Red staining. *B. distachyon* dry grains were first treated with fixation buffer (4% [v/v] paraformaldehyde and 0.25% [v/v] glutaraldehyde in phosphate-buffered saline [PBS], pH 7), then stained with 0.1% (w/v) Nile Red (Molecular Probes) in acetone for 20 min at room temperature, and briefly rinsed with PBS buffer (8.0 g L^{-1} NaCl, 0.2 g L^{-1} KCl, 1.44 g L^{-1} Na_2HPO_4, and 0.24 g L^{-1} KH_2PO_4, pH 7.4). *B. distachyon* leaf blades and internodes were directly stained with 0.1% (w/v) Nile Red for 20 min at room temperature without fixation and briefly rinsed with PBS buffer. Neutral lipids were observed using an Olympus FluoView 1000 Laser Scanning Confocal Microscope with excitation at 488 nm and emission at 550 to 670 nm. The number and size of lipid droplets in *B. distachyon* grains were measured using Fluoview Viewer (Olympus).

ROS production was analyzed using H_2DCF-DA (Invitrogen) following the manufacturer's manual. Detached leaf tissues from 8-week-old *B. distachyon* or 4-week-old Arabidopsis were incubated in H_2DCF-DA staining buffer (10 μM H_2DCF-DA in PBS buffer). Vacuum was applied for 20 min followed by staining for 20 min at room temperature. After staining, the tissues were briefly washed with PBS buffer. The fluorescence signal was detected using an Olympus FluoView 1000 Laser Scanning Confocal Microscope with excitation at 488 nm and emission at 535 nm.

Production of H_2O_2 was examined following staining with DAB. *B. distachyon* leaf blades (8 weeks old) were harvested and immersed in 1 mg mL^{-1} DAB solution (pH 3.8). Vacuum was applied for 20 min followed by staining for 8 h in the dark at room temperature. After staining, samples were cleared with clearing buffer (ethanol:acetic acid:glycerol, 3:3:1, v/v) at 95°C. Samples were examined using a Leica MZ125 microscope.

FA Treatment

The 18:2 and 16:0 FAs and cerulenin were purchased from Sigma and dissolved in ethanol. FA treatment was performed as described (Fan et al., 2013), with minor modifications. Detached 3-week-old *B. distachyon* leaf blades were floated in water containing 0.0005% (v/v) Tween 20, 0.25% (v/v) ethanol, and

various concentrations of free FAs (0, 50, 100, or 200 μM) in light. The control was treated with water containing 0.0005% (v/v) Tween 20 and 0.25% (v/v) ethanol. Cerulenin was added at a final concentration of 5 μg mL^{-1}.

The Arabidopsis Genome Initiative locus identifiers (https://www.arabidopsis.org/) used in this study are as follows: *At3g54230* (*AtWRI1*), *At5g04040* (*AtSDP1*), *At4g16760* (*AtACX1*), *At5g65110* (*AtACX2*), *At3g05970* (*AtLACS6*), *At5g27600* (*AtLACS7*), *At1g04710* (*AtKAT1*), *At2g33150* (*AtKAT2*), *At3g06860* (*AtMFP2*), and *At2g37620* (*AtACTIN1*). Accession numbers for *B. distachyon* locus identifiers (http://www.phytozome.net/) are as follows: *Brai4g43877* (*BdWRI1*), *Bradi2g45620* (*BdPKPβ1*), *Bradi1g46610* (*BdKASI*), *Bradi1g01000* (*BdACP1*), *Bradi2g50610* (*BdSDP1-1*), *Bradi1g04310* (*BdSDP1-2*), *Bradi1g52320* (*BdACX1*), *Bradi4g14090* (*BdACX2*), *Bradi4g26610* (*BdLACS6*), *Bradi4g42950* (*BdLACS7*), *Bradi2g43020* (*BdMFP2-1*), *Bradi4g28310* (*BdMFP2-2*), *Bradi4g28310* (*BdMFP2-3*), *Bradi3g27960* (*BdKAT1*), *Bradi3g55420* (*BdKAT2*), and *Bradi4g00660* (*BdUBC18*). Accession numbers for all the AP2-containing proteins in *B. distachyon* were obtained from Phytozome (https://www.arabidopsis.org/) and are shown in Figure 1.

Supplemental Data

The following supplemental materials are available.

Supplemental Figure S1. Alignment of WRI1 amino acid sequences from *B. distachyon* and Arabidopsis.

Supplemental Figure S2. Lipid droplets are abundant in embryo and endosperm of *UBI::BdWRI1* line 5A dry grains.

Supplemental Figure S3. Lipid droplets in the internodes of *UBI::BdWRI1* plants.

Supplemental Figure S4. Ectopic expression of *AtWRI1* also led to cell death in *B. distachyon*.

Supplemental Figure S5. Ectopic expression of *AtWRI1* in Arabidopsis did not lead to cell death.

Supplemental Figure S6. No induction of TAG turnover in *35S::AtWRI1* vegetative tissues of Arabidopsis.

Supplemental Figure S7. Palmitic acid (16:0) treatment of *B. distachyon* leaf blade results in cell death.

Supplemental Table S1. PCR primers used in RT-PCR.

ACKNOWLEDGMENTS

We thank Dr. Henrik Tjellström (Michigan State University) for advice on lipid analysis and FA treatments, Dr. Sarah Gilmour (Michigan State University) for advice on electrolyte leakage measurement, and Dr. Melinda Frame (Michigan State University Center for Advanced Microscopy) for confocal microscopy experiments.

Received August 6, 2015; accepted September 25, 2015; published September 29, 2015.

LITERATURE CITED

Ando T, Tsukamotoa Y (1981) Inhibitory action of saturated fatty acids and their derivatives. Phytochemistry **20:** 2143–2144

Andre C, Haslam RP, Shanklin J (2012) Feedback regulation of plastidic acetyl-CoA carboxylase by 18:1-acyl carrier protein in *Brassica napus*. Proc Natl Acad Sci USA **109:** 10107–10112

Apel K, Hirt H (2004) Reactive oxygen species: metabolism, oxidative stress, and signal transduction. Annu Rev Plant Biol **55:** 373–399

Awaya J, Ohno T, Ohno H, Omura S (1975) Substitution of cellular fatty acids in yeast cells by the antibiotic cerulenin and exogenous fatty acids. Biochim Biophys Acta **409:** 267–273

Baker CJ, Orlandi EW (1995) Active oxygen in plant pathogenesis. Annu Rev Phytopathol **33:** 299–321

Bates PD, Browse J (2011) The pathway of triacylglycerol synthesis through phosphatidylcholine in Arabidopsis produces a bottleneck for the accumulation of unusual fatty acids in transgenic seeds. Plant J **68:** 387–399

Bates PD, Browse J (2012) The significance of different diacylgycerol synthesis pathways on plant oil composition and bioengineering. Front Plant Sci **3:** 147

Bates PD, Fatihi A, Snapp AR, Carlsson AS, Browse J, Lu C (2012) Acyl editing and headgroup exchange are the major mechanisms that direct polyunsaturated fatty acid flux into triacylglycerols. Plant Physiol **160:** 1530–1539

Bates PD, Ohlrogge JB, Pollard M (2007) Incorporation of newly synthesized fatty acids into cytosolic glycerolipids in pea leaves occurs via acyl editing. J Biol Chem **282:** 31206–31216

Bates PD, Stymne S, Ohlrogge J (2013) Biochemical pathways in seed oil synthesis. Curr Opin Plant Biol **16:** 358–364

Baud S, Lepiniec L (2010) Physiological and developmental regulation of seed oil production. Prog Lipid Res **49:** 235–249

Baud S, Wuillème S, To A, Rochat C, Lepiniec L (2009) Role of WRINKLED1 in the transcriptional regulation of glycolytic and fatty acid biosynthetic genes in Arabidopsis. Plant J **60:** 933–947

Baxter A, Mittler R, Suzuki N (2014) ROS as key players in plant stress signalling. J Exp Bot **65:** 1229–1240

Berrie AM (1979) Possible role of volatile fatty acids and abscisic acid in the dormancy of oats. Plant Physiol **63:** 758–764

Bosma R, Miazek K, Willemsen SM, Vermuë MH, Wijffels RH (2008) Growth inhibition of Monodus subterraneus by free fatty acids. Biotechnol Bioeng **101:** 1108–1114

Brkljacic J, Grotewold E, Scholl R, Mockler T, Garvin DF, Vain P, Brutnell T, Sibout R, Bevan M, Budak H, et al (2011) Brachypodium as a model for the grasses: today and the future. Plant Physiol **157:** 3–13

Cernac A, Andre C, Hoffmann-Benning S, Benning C (2006) WRI1 is required for seed germination and seedling establishment. Plant Physiol **141:** 745–757

Cernac A, Benning C (2004) *WRINKLED1* encodes an AP2/EREB domain protein involved in the control of storage compound biosynthesis in Arabidopsis. Plant J **40:** 575–585

Chandra-Shekara AC, Venugopal SC, Barman SR, Kachroo A, Kachroo P (2007) Plastidial fatty acid levels regulate resistance gene-dependent defense signaling in Arabidopsis. Proc Natl Acad Sci USA **104:** 7277–7282

Danon A, Miersch O, Felix G, Camp RG, Apel K (2005) Concurrent activation of cell death-regulating signaling pathways by singlet oxygen in Arabidopsis thaliana. Plant J **41:** 68–80

Dellagi A, Brisset MN, Paulin JP, Expert D (1998) Dual role of desferrioxamine in Erwinia amylovora pathogenicity. Mol Plant Microbe Interact **11:** 734–742

del Rio LA, Pastori GM, Palma JM, Sandalio LM, Sevilla F, Corpas FJ, Jimenez A, Lopez-Huertas E, Hernandez JA (1998) The activated oxygen role of peroxisomes in senescence. Plant Physiol **116:** 1195–1200

Draper J, Mur LA, Jenkins G, Ghosh-Biswas GC, Bablak P, Hasterok R, Routledge AP (2001) *Brachypodium distachyon*: a new model system for functional genomics in grasses. Plant Physiol **127:** 1539–1555

Durrett TP, Benning C, Ohlrogge J (2008) Plant triacylglycerols as feedstocks for the production of biofuels. Plant J **54:** 593–607

Dussert S, Guerin C, Andersson M, Joët T, Tranbarger TJ, Pizot M, Sarah G, Omore A, Durand-Gasselin T, Morcillo F (2013) Comparative transcriptome analysis of three oil palm fruit and seed tissues that differ in oil content and fatty acid composition. Plant Physiol **162:** 1337–1358

Eastmond PJ (2006) *SUGAR-DEPENDENT1* encodes a patatin domain triacylglycerol lipase that initiates storage oil breakdown in germinating *Arabidopsis* seeds. Plant Cell **18:** 665–675

Eastmond PJ (2007) *MONODEHYROASCORBATE REDUCTASE4* is required for seed storage oil hydrolysis and postgerminative growth in *Arabidopsis*. Plant Cell **19:** 1376–1387

Fakas S, Qiu Y, Dixon JL, Han GS, Ruggles KV, Garbarino J, Sturley SL, Carman GM (2011) Phosphatidate phosphatase activity plays key role in protection against fatty acid-induced toxicity in yeast. J Biol Chem **286:** 29074–29085

Fan J, Yan C, Roston R, Shanklin J, Xu C (2014) *Arabidopsis* lipins, PDAT1 acyltransferase, and SDP1 triacylglycerol lipase synergistically direct fatty acids toward β-oxidation, thereby maintaining membrane lipid homeostasis. Plant Cell **26:** 4119–4134

Fan J, Yan C, Xu C (2013) Phospholipid:diacylglycerol acyltransferase-mediated triacylglycerol biosynthesis is crucial for protection against

fatty acid-induced cell death in growing tissues of Arabidopsis. Plant J **76:** 930–942

Farmer EE, Weber H, Vollenweider S (1998) Fatty acid signaling in Arabidopsis. Planta **206:** 167–174

Focks N, Benning C (1998) *wrinkled1*: a novel, low-seed-oil mutant of Arabidopsis with a deficiency in the seed-specific regulation of carbohydrate metabolism. Plant Physiol **118:** 91–101

Fryer MJ, Oxborough K, Mullineaux PM, Baker NR (2002) Imaging of photo-oxidative stress responses in leaves. J Exp Bot **53:** 1249–1254

Fukuda N, Ikawa Y, Aoyagi T, Kozaki A (2013) Expression of the genes coding for plastidic acetyl-CoA carboxylase subunits is regulated by a location-sensitive transcription factor binding site. Plant Mol Biol **82:** 473–483

Garbarino J, Padamsee M, Wilcox L, Oelkers PM, D'Ambrosio D, Ruggles KV, Ramsey N, Jabado O, Turkish A, Sturley SL (2009) Sterol and diacylglycerol acyltransferase deficiency triggers fatty acid-mediated cell death. J Biol Chem **284:** 30994–31005

Gilmour SJ, Hajela RK, Thomashow MF (1988) Cold acclimation in *Arabidopsis thaliana*. Plant Physiol **87:** 745–750

Goepfert S, Poirier Y (2007) Beta-oxidation in fatty acid degradation and beyond. Curr Opin Plant Biol **10:** 245–251

Golbeck JH, Warden JT (1984) Interaction of linolenic acid with bound quinone molecules in photosystem II: time-resolved optical and electron spin resonance studies. Biochim Biophys Acta **767:** 263–271

Graham IA (2008) Seed storage oil mobilization. Annu Rev Plant Biol **59:** 115–142

Graham IA, Eastmond PJ (2002) Pathways of straight and branched chain fatty acid catabolism in higher plants. Prog Lipid Res **41:** 156–181

Grimberg A, Carlsson AS, Marttila S, Bhalerao R, Hofvander P (2015) Transcriptional transitions in Nicotiana benthamiana leaves upon induction of oil synthesis by WRINKLED1 homologs from diverse species and tissues. BMC Plant Biol **15:** 192

Guillon F, Larré C, Petipas F, Berger A, Moussawi J, Rogniaux H, Santoni A, Saulnier L, Jamme F, Miquel M, et al (2012) A comprehensive overview of grain development in Brachypodium distachyon variety Bd21. J Exp Bot **63:** 739–755

Heneen WK, Karlsson G, Brismar K, Gummeson PO, Marttila S, Leonova S, Carlsson AS, Bafor M, Banas A, Mattsson B, et al (2008) Fusion of oil bodies in endosperm of oat grains. Planta **228:** 589–599

Himmelbach A, Zierold U, Hensel G, Riechen J, Douchkov D, Schweizer P, Kumlehn J (2007) A set of modular binary vectors for transformation of cereals. Plant Physiol **145:** 1192–1200

Hofius D, Schultz-Larsen T, Joensen J, Tsitsigiannis DI, Petersen NH, Mattsson O, Jørgensen LB, Jones JD, Mundy J, Petersen M (2009) Autophagic components contribute to hypersensitive cell death in Arabidopsis. Cell **137:** 773–783

Hong SY, Seo PJ, Yang MS, Xiang F, Park CM (2008) Exploring valid reference genes for gene expression studies in Brachypodium distachyon by real-time PCR. BMC Plant Biol **8:** 112

Kachroo A, Lapchyk L, Fukushige H, Hildebrand D, Klessig D, Kachroo P (2003) Plastidial fatty acid signaling modulates salicylic acid- and jasmonic acid-mediated defense pathways in the *Arabidopsis ssi2* mutant. Plant Cell **15:** 2952–2965

Kelly AA, van Erp H, Quettier AL, Shaw E, Menard G, Kurup S, Eastmond PJ (2013) The SUGAR-DEPENDENT1 lipase limits triacylglycerol accumulation in vegetative tissues of Arabidopsis. Plant Physiol **162:** 1282–1289

Kohlwein SD (2010) Triacylglycerol homeostasis: insights from yeast. J Biol Chem **285:** 15663–15667

Koo AJ, Fulda M, Browse J, Ohlrogge JB (2005) Identification of a plastid acyl-acyl carrier protein synthetase in Arabidopsis and its role in the activation and elongation of exogenous fatty acids. Plant J **44:** 620–632

Kunz HH, Scharnewski M, Feussner K, Feussner I, Flügge UI, Fulda M, Gierth M (2009) The ABC transporter PXA1 and peroxisomal β-oxidation are vital for metabolism in mature leaves of *Arabidopsis* during extended darkness. Plant Cell **21:** 2733–2749

Lee JN, Kim H, Yao H, Chen Y, Weng K, Ye J (2010) Identification of Ubxd8 protein as a sensor for unsaturated fatty acids and regulator of triglyceride synthesis. Proc Natl Acad Sci USA **107:** 21424–21429

Le Poidevin N (1965) Inhibition of the germination of mustard seeds by saturated fatty acids. Phytochemistry **4:** 525–526

Li M, Bahn SC, Guo L, Musgrave W, Berg H, Welti R, Wang X (2011) Patatin-related phospholipase pPLAIIIβ-induced changes in lipid metabolism alter cellulose content and cell elongation in *Arabidopsis*. Plant Cell **23:** 1107–1123

Liu J, Hua W, Zhan G, Wei F, Wang X, Liu G, Wang H (2010) Increasing seed mass and oil content in transgenic Arabidopsis by the overexpression of *wri1-like* gene from *Brassica napus*. Plant Physiol Biochem **48:** 9–15

Livak KJ, Schmittgen TD (2001) Analysis of relative gene expression data using real-time quantitative PCR and the $2^{-\text{Delta Delta C(T)}}$ Method. Methods **25:** 402–408

Ma W, Kong Q, Arondel V, Kilaru A, Bates PD, Thrower NA, Benning C, Ohlrogge JB (2013) Wrinkled1, a ubiquitous regulator in oil accumulating tissues from Arabidopsis embryos to oil palm mesocarp. PLoS One **8:** e68887

Ma W, Kong Q, Grix M, Mantyla JJ, Yang Y, Benning C, Ohlrogge JB (2015) Deletion of a C-terminal intrinsically disordered region of WRINKLED1 affects its stability and enhances oil accumulation in Arabidopsis. Plant J **83:** 864–874

Maeo K, Tokuda T, Ayame A, Mitsui N, Kawai T, Tsukagoshi H, Ishiguro S, Nakamura K (2009) An AP2-type transcription factor, WRINKLED1, of *Arabidopsis thaliana* binds to the AW-box sequence conserved among proximal upstream regions of genes involved in fatty acid synthesis. Plant J **60:** 476–487

Meng Y, Li H, Wang Q, Liu B, Lin C (2013) Blue light-dependent interaction between cryptochrome2 and CIB1 regulates transcription and leaf senescence in soybean. Plant Cell **25:** 4405–4420

Metzger JD, Sebesta DK (1982) Role of endogenous growth regulators in seed dormancy of *Avena fatua*. I. Short chain fatty acids. Plant Physiol **70:** 1480–1485

Miquel M, Trigui G, d'Andréa S, Kelemen Z, Baud S, Berger A, Deruyffelaere C, Trubuil A, Lepiniec L, Dubreucq B (2014) Specialization of oleosins in oil body dynamics during seed development in Arabidopsis seeds. Plant Physiol **164:** 1866–1878

Murashige T, Skoog F (1962) A revised medium for rapid growth and bioassays with tobacco tissue cultures. Physiol Plant **15:** 473–497

Ohkawa M, Nishikawa Y (1987) Plant growth inhibitory activity of fatty acids and the related compounds by the Avena coleoptile test. Plant Sci **53:** 35–38

Ohlrogge J, Chapman K (2011) The seeds of green energy: expanding the contribution of plant oils as biofuels. Biochemist (Lond) **33:** 34–38

Opanowicz M, Vain P, Draper J, Parker D, Doonan JH (2008) Brachypodium distachyon: making hay with a wild grass. Trends Plant Sci **13:** 172–177

Packter NM, Stumpf PK (1975) Fat metabolism in higher plants: the effect of cerulenin on the synthesis of medium- and long-chain acids in leaf tissue. Arch Biochem Biophys **167:** 655–667

Padham AK, Hopkins MT, Wang TW, McNamara LM, Lo M, Richardson LG, Smith MD, Taylor CA, Thompson JE (2007) Characterization of a plastid triacylglycerol lipase from Arabidopsis. Plant Physiol **143:** 1372–1384

Penfield S, Rylott EL, Gilday AD, Graham S, Larson TR, Graham IA (2004) Reserve mobilization in the *Arabidopsis* endosperm fuels hypocotyl elongation in the dark, is independent of abscisic acid, and requires *PHOSPHOENOLPYRUVATE CARBOXYKINASE1*. Plant Cell **16:** 2705–2718

Peters J, Chin CK (2007) Potassium loss is involved in tobacco cell death induced by palmitoleic acid and ceramide. Arch Biochem Biophys **465:** 180–186

Peters JS, Chin C (2005) Evidence for cytochrome f involvement in eggplant cell death induced by palmitoleic acid. Cell Death Differ **12:** 405–407

Peters JS, Chin CK (2003) Inhibition of photosynthetic electron transport by palmitoleic acid is partially correlated to loss of thylakoid membrane proteins. Plant Physiol Biochem **41:** 117–124

Pouvreau B, Baud S, Vernoud V, Morin V, Py C, Gendrot G, Pichon JP, Rouster J, Paul W, Rogowsky PM (2011) Duplicate maize *Wrinkled1* transcription factors activate target genes involved in seed oil biosynthesis. Plant Physiol **156:** 674–686

Qu J, Ye J, Geng YF, Sun YW, Gao SQ, Zhang BP, Chen W, Chua NH (2012) Dissecting functions of *KATANIN* and *WRINKLED1* in cotton fiber development by virus-induced gene silencing. Plant Physiol **160:** 738–748

Ramel F, Sulmon C, Bogard M, Couée I, Gouesbet G (2009) Differential patterns of reactive oxygen species and antioxidative mechanisms

during atrazine injury and sucrose-induced tolerance in Arabidopsis thaliana plantlets. BMC Plant Biol **9:** 28

Roudier F, Gissot L, Beaudoin F, Haslam R, Michaelson L, Marion J, Molino D, Lima A, Bach L, Morin H, et al (2010) Very-long-chain fatty acids are involved in polar auxin transport and developmental patterning in *Arabidopsis*. Plant Cell **22:** 364–375

Roughan PG, Thompson GA Jr, Cho SH (1987) Metabolism of exogenous long-chain fatty acids by spinach leaves. Arch Biochem Biophys **259:** 481–496

Sanjaya, Durrett TP, Weise SE, Benning C (2011) Increasing the energy density of vegetative tissues by diverting carbon from starch to oil biosynthesis in transgenic Arabidopsis. Plant Biotechnol J **9:** 874–883

Sanjaya, Miller R, Durrett TP, Kosma DK, Lydic TA, Muthan B, Koo AJ, Bukhman YV, Reid GE, Howe GA, et al (2013) Altered lipid composition and enhanced nutritional value of *Arabidopsis* leaves following introduction of an algal diacylglycerol acyltransferase 2. Plant Cell **25:** 677–693

Santos-Mendoza M, Dubreucq B, Baud S, Parcy F, Caboche M, Lepiniec L (2008) Deciphering gene regulatory networks that control seed development and maturation in Arabidopsis. Plant J **54:** 608–620

Schmitt FJ, Renger G, Friedrich T, Kreslavski VD, Zharmukhamedov SK, Los DA, Kuznetsov VV, Allakhverdiev SI (2014) Reactive oxygen species: re-evaluation of generation, monitoring and role in stress-signaling in phototrophic organisms. Biochim Biophys Acta **1837:** 835–848

Shen B, Allen WB, Zheng P, Li C, Glassman K, Ranch J, Nubel D, Tarczynski MC (2010) Expression of *ZmLEC1* and *ZmWRI1* increases seed oil production in maize. Plant Physiol **153:** 980–987

Shintani DK, Ohlrogge JB (1995) Feedback inhibition of fatty acid synthesis in tobacco suspension cells. Plant J **7:** 577–587

Slocombe SP, Cornah J, Pinfield-Wells H, Soady K, Zhang Q, Gilday A, Dyer JM, Graham IA (2009) Oil accumulation in leaves directed by modification of fatty acid breakdown and lipid synthesis pathways. Plant Biotechnol J **7:** 694–703

Stewart RR, Berrie AM (1979) Effect of temperature on the short chain fatty acid-induced inhibition of lettuce seed germination. Plant Physiol **63:** 61–62

Tamura K, Stecher G, Peterson D, Filipski A, Kumar S (2013) MEGA6: Molecular Evolutionary Genetics Analysis version 6.0. Mol Biol Evol **30:** 2725–2729

Terzaghi WB (1986) Metabolism of Tween-fatty acid esters by cultured soybean cells: kinetics of incorporation into lipids, subsequent turnover, and associated changes in endogenous fatty acid synthesis. Plant Physiol **82:** 780–786

Tjellström H, Strawsine M, Ohlrogge JB (2015) Tracking synthesis and turnover of triacylglycerol in leaves. J Exp Bot **66:** 1453–1461

Torres MA, Dangl JL, Jones JD (2002) Arabidopsis gp91phox homologues AtrbohD and AtrbohF are required for accumulation of reactive oxygen intermediates in the plant defense response. Proc Natl Acad Sci USA **99:** 517–522

Tranbarger TJ, Dussert S, Joët T, Argout X, Summo M, Champion A, Cros D, Omore A, Nouy B, Morcillo F (2011) Regulatory mechanisms underlying oil palm fruit mesocarp maturation, ripening, and functional specialization in lipid and carotenoid metabolism. Plant Physiol **156:** 564–584

Tso TC (1964) Plant-growth inhibition by some fatty acids and their analogues. Nature **202:** 511–512

Tsuzuki E, Yamamoto Y, Shimizu T (1987) Fatty acids in buckwheat are growth inhibitors. Ann Bot (Lond) **60:** 69–70

van Erp H, Kelly AA, Menard G, Eastmond PJ (2014) Multigene engineering of triacylglycerol metabolism boosts seed oil content in Arabidopsis. Plant Physiol **165:** 30–36

Vanhercke T, El Tahchy A, Liu Q, Zhou XR, Shrestha P, Divi UK, Ral JP, Mansour MP, Nichols PD, James CN, et al (2014) Metabolic engineering of biomass for high energy density: oilseed-like triacylglycerol yields from plant leaves. Plant Biotechnol J **12:** 231–239

Vanhercke T, El Tahchy A, Shrestha P, Zhou XR, Singh SP, Petrie JR (2013) Synergistic effect of WRI1 and DGAT1 coexpression on triacylglycerol biosynthesis in plants. FEBS Lett **587:** 364–369

Vogel J, Hill T (2008) High-efficiency Agrobacterium-mediated transformation of Brachypodium distachyon inbred line Bd21-3. Plant Cell Rep **27:** 471–478

Wang Z, Benning C (2011) Arabidopsis thaliana polar glycerolipid profiling by thin layer chromatography (TLC) coupled with gas-liquid chromatography (GLC). J Vis Exp **49:** 2518

Warden JT, Csatorday K (1987) On the mechanism of linolenic acid inhibition in photosystem II. Biochim Biophys Acta **890:** 215–223

Wu JT, Chiang YR, Huang WY, Jane WN (2006) Cytotoxic effects of free fatty acids on phytoplankton algae and cyanobacteria. Aquat Toxicol **80:** 338–345

Zhang D, Yuan Z (2014) Molecular control of grass inflorescence development. Annu Rev Plant Biol **65:** 553–578